Hyperfine Interact (2018) 239: 28
https://doi.org/10.1007/s10751-018-1498-y

Mössbauer characterisation of synthetic analogues of the helvite minerals $Fe_4M_4[BeSiO_4]_6X_2$ (M = Fe, Mn, Zn; X = S, Se)

Sandra E. Dann[1] · Klaus U. Neumann[2] · José F. Marco[3]

Published online: 9 July 2018

Abstract We report on this paper on the Mössbauer characterisation of the family of synthetic helvite analogues, $Fe_4M_4[BeSiO_4]_6X_2$ (M = Fe, Mn, Zn; X = S, Se). The data show iron to be present as high spin Fe(II) in tetrahedral coordination. The room temperature Mössbauer spectra are composed either by singlets or doublets with small quadrupole splitting values suggesting a small valence contribution at that temperature. From the dependence of the quadrupole splitting with temperature the separation Δ between the two e_g orbitals has been estimated. The values of Δ range from 46.3 cm^{-1} for the material $Fe_8[BeSiO_4]_6S_2$ to 58.2 cm^1 for the material $Fe_4Zn_4[BeSiO_4]_6S_2$. The lack of long-range magnetic order observed in the Mössbauer spectra was confirmed by neutron diffraction data which suggests that the M_4X units are largely magnetically isolated within their cages leading to a frustrated magnet with no long range interaction for the sulfide species.

Keywords Danalite · Helvite · Mössbauer spectroscopy · Magnetic properties

This article is part of the Topical Collection on *Proceedings of the 4th Mediterranean Conference on the Applications of the Mössbauer Effect (MECAME 2018), Zadar, Croatia, 27–31 May 2018*
Edited by Mira Ristic and Stjepko Krehula

✉ José F. Marco
jfmarco@iqfr.csic.es

Sandra E. Dann
s.e.dann@lboro.ac.uk

Klaus U. Neumann
k.u.neumann@lboro.ac.uk

[1] Department of Chemistry, Loughbourough University, Leicestershire LE11 3TU, UK

[2] Department of Physics, Loughbourough University, Leicestershire LE11 3TU, UK

[3] Instituto de Química-Física "Rocasolano", CSIC, c/ Serrano, 119, 28006 Madrid, Spain

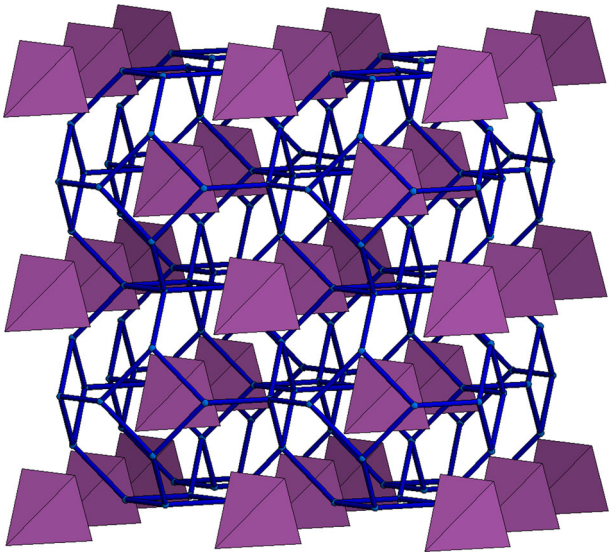

Fig. 1 Structure of $M_8[BeSiO_4]_6X_2$ showing the M_4X Tetrahedra. Metal chalcogenide tetrahedra (lilac) embedded in a $(T,T')O_2$ framework. Oxygen is omitted for clarity and T-T links are shown (blue)

1 Introduction

The helvite group of minerals, with formula $(Fe,Mn,Zn)_8(BeSiO_4)_6S_2$, exist in nature within a significant compositional range of iron, manganese and zinc depending on the geology of the region where they occur. While the zinc (genthelvite) and manganese [1] end members exist in nature and have been prepared synthetically using 2kbr hydrothermal pressure and 750 °C [2], the pure iron species (danalite) does not occur geologically and had not been prepared using high pressure hydrothermal synthesis. Using high temperature in the laboratory, it has been possible to prepare the iron-rich materials in the laboratory, control their stoichometry and also prepare selenium and tellurium analogues [3]. The materials crystallise wth the sodalite structure, with a framework of vertex-sharing alternating beryllium and silicon tetrahedra, at the centre of the sodalite cage lies an M_4X tetrahedron (M = Fe, Mn and Zn) and X = S, Se or Te. The metal ions are tetrahedrally coordinated to three framework oxygens and the central chalcogen giving the metal species a tetrahedral coordination (Fig. 1). This leads to an ordered array of tetrahedral M_4X clusters within the framework. Since the transition metal cations within the cluster contain unpaired electrons, this leads to the possibility of unusual magnetic interactions; since antiferromagnetic pairwise exchange cannot be satisfied in all three directions simultaneously in a tetrahedron, it leads to the possibility of magnetic frustration. Previous work on the manganese analogue showed strong interactions within the manganese clusters with a paramagnetic Curie temperature of 100 K, however no Neel temperature was observed down to 4.2 K [4] indicating strong coupling within cages but no coupling between them. The difference in the strength of interaction presumably results from the distances over which such interactions take place. These dimensions for a typical sodalite, such as danalite, $Fe_8[BeSiO_4]_6S_2$, are shown in Fig. 2. In this material, consideration of the iron-iron separations within the cage, intra-cage (3.93 Å) and inter-cage (4.54 Å) indicates why the strength of these interactions may be different. In addition, there is the possibility for a through bond interaction via

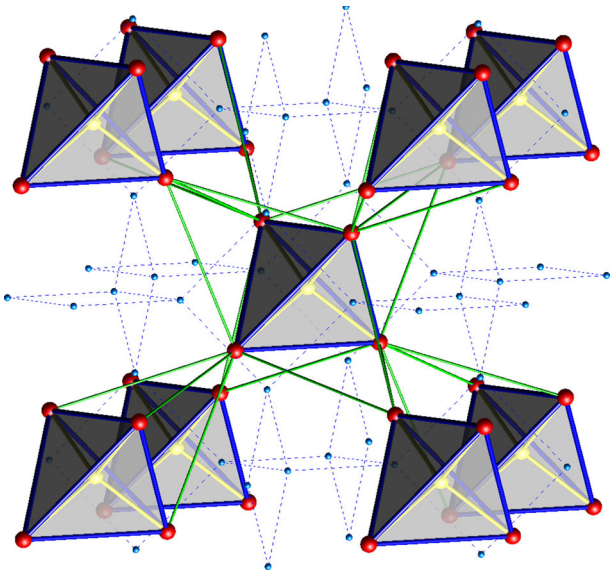

Fig. 2 Interactions in the Danalite Structure. The Fe_4S tetrahedral units (shaded tetrahedra), intracage Fe-Fe distances (blue) and intercage Fe-Fe distances (green) are shown. The framework is shown as dotted T-T distances (blue)

sulphur within a sodalite cage, while the intercage interaction would have to proceed via one or more framework oxygen atoms. Thus for electronically and magnetically active centres, the possibility exists for two distinct types of interaction—local for the four metal centres within a sodalite cage and a true long-range three- dimensional interaction between the units within the cages. The ability to prepare iron containing analogues of these materials means that Mössbauer could be used to further probe the local structure and interaction between the units. This paper reports the results of low temperature experimental investigations on these materials by Mössbauer spectroscopy and magnetic measurements.

2 Experimental

For the synthesis of the materials, the method previously described for tellurite aluminate sodalite was followed. BeO, SiO_2, powdered Fe and X (X = S, Se) were homogeneously ground using an agate pestle and mortar in an argon-filled glove box (1 ppm water/ 1 pppm oxygen). The mixtures were placed in quartz tubes, evacuated and sealed. The tubes were heated in the centre of a tube furnace fitted with inconel work tube in stages up to 1100C and maintained at this temperature for 48 h. The samples were slow cooled and transferred back to the glove box where they were opened with a glass cutter. Samples were ground and placed in plastic sample holders and sealed under mylar film due to the toxicity of beryllium oxide for x-ray diffraction analysis. EDX was performed on powdered samples and gave good agreement for the Fe:Si:X ratios [Fe:Si:S was 1.82:0.88:0.29 or 6:3:1] (quantification of Be is not possible due to the low atomic number)). Samples were ground and placed in plastic sample holders and sealed under mylar film due to the toxicity of beryllium oxide for x-ray diffraction analysis.

Mössbauer spectra were recorded using a conventional constant acceleration spectrometer with a ^{57}Co(Rh) source. The absorbers were prepared to contain an amount of natural Fe of about 8–10 mg cm^{-2}. Low temperature Mössbauer spectra were recorded using a He-closed cycle cryogenerator. All the spectra were computer fitted and the isomer shifts referred to the centroid of the spectrum of α-iron at room temperature.

Magnetic measurements were carried out on $Fe_8[BeSiO_4]_6S_2$ and $Fe_4Mn_4[BeSiO_4]_6S_2$ using a SQUID magnetometer in the temperature range 2 K to 310 K using fields up to 5.5 Tesla.

Paramagnetic neutron scattering experiments were carried out on D7 at the ILL (Grenoble, France) and on the instrument DNS at the IFF in Jülich (Germany). The magnetic scattering signatures of the cluster compounds $Fe(BeSiO_4)_6X_2$ with X = S, Se were investigated. The magnetic scattering cross-section was measured as a function of Q through an XYZ polarisation analysis. Data were collected at 200, 50, 20, 10, 5 and 2 K for $Fe_8(BeSiO_4)_6S_2$ and a similar set of temperatures for $Fe_8(BeSiO_4)_6Se_2$. Normal data reduction methods were applied to extract the magnetic contribution to the total scattering, see for example http://www.ill.fr/YellowBook/D7/home/homeindex.html, producing plots of the magnetic cross section as a function of wave-vector transfer (Q).

3 Results and discussion

The Mössbauer spectra recorded from the iron-rich samples are shown in Fig. 3. The Mössbauer parameters obtained from the fits to the spectra are collected in Table 1. The $Fe_8[BeSiO_4]_6S_2$ and $Fe_8[BeSiO_4]_6$ Se_2 Mössbauer spectra consist of a main contribution that accounts for 97% of the total spectral area and a minor quadrupole doublet that accounts for 3% of the total spectral area. The latter is associated with a minor impurity phase of poor crystallinity (probably fayalite) which does not show up in the powder diffraction pattern. The isomer shift (δ) of the main contribution in all the samples is centred at 0.93 mm s^{-1} which is consistent with high spin iron(II) in a tetrahedral environment [5]. The quadrupole splitting (ΔE_Q) shown by the main absorptions increases as the size of the chalcogenide increases. It is widely accepted that for high spin iron(II) species, the contribution of the valence electrons to the electric field gradient (EFG) is usually much higher than that due to the contribution of the lattice. In the case of the iron sulfide material, there is zero quadrupole splitting. A zero quadrupole splitting would only be expected if the anions surrounding the iron(II) ion were identical. The sixth electron of the high spin iron(II) would then be equally distributed between the degenerate e_g orbitals (dx^2-y^2 and dz^2) and the contribution of the valence electrons to the electric field gradient would be zero. However, in the danalite family of minerals, the iron(II) ion is not in a perfect tetrahedral environment since it is coordinated to three oxygens from the framework and to the central chalcogenide anion. The elongated tetrahedral geometry and consequential loss of degeneracy of the e_g orbitals should result in a significant contribution of the valence electrons to the electric field gradient where the sixth electron would now occupy either dx^2-y^2 or dz^2 preferentially. It is also well known that the valence and lattice contributions to the EFG are of opposite sign [6]. This implies that at room temperature the lattice contribution to the electric field gradient (which is independent of temperature) must be large enough to exactly compensate for the lattice contribution. This finding is remarkable as it suggests that the separation of the two e states brought about by the elongated tetrahedral symmetry in the case of the sulfide is very small. To evaluate the separation Δ between the two e_g states split by the effect of tetragonal distortion (Fig. 4), series of low temperature were recorded.

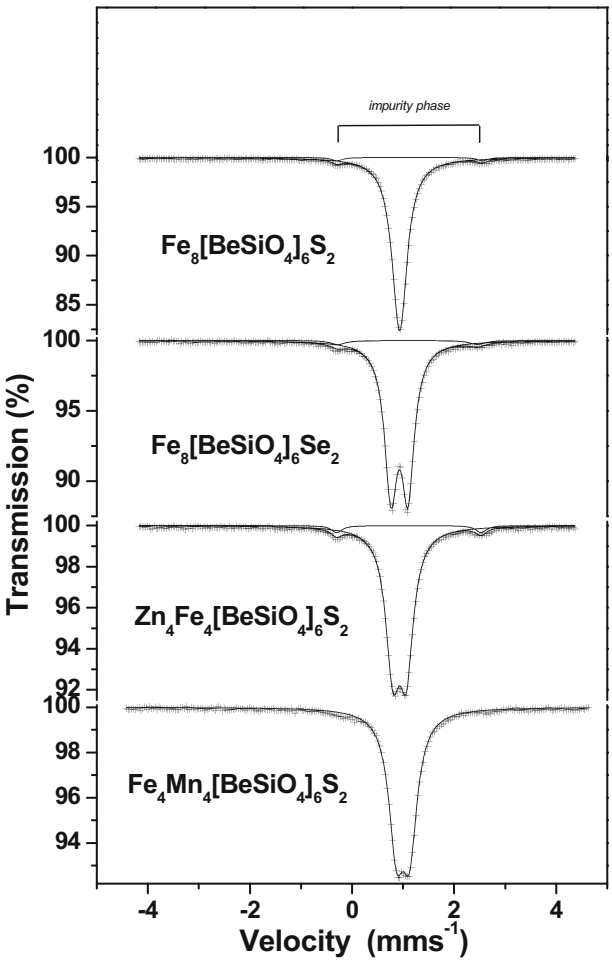

Fig. 3 Room temperature Mössbauer spectra recorded from the different samples

Figure 5 shows the Mössbauer spectra recorded from $Fe_8[BeSiO_4]_6S_2$ in the range 15–298 K. inspection of Fig. 5 shows how the singlet observed at room temperature transforms into a doublet with decreasing temperature. The separation between the two lines of the doublet also increases with decreasing temperature as it should be expected for a high spin Fe(II) species. It is also observed (Fig. 6) that the linewidth of the doublet increases from the value of 0.36 mms^{-1} at room temperature up to *ca.* 0.90 mms^{-1} at 60 K and then it decreases to *ca.* 0.36 mms^{-1} again at 15 K. This behaviour which has been observed previously in a natural dalanite sample of formula formula $Fe_{1.94}Mn_{1.58}Zn_{0.39}Ca_{0.09}[BeSiO_4]_6S_2$ [7], suggests the existence of a distribution of quadrupole splittings. This may be originated by small geometrical distortions of the Fe(II)-O tetrahedra which bring about small differences in the crystal field strength. In other words, the separation Δ between the two e_g states might not be the exactly the same at a given intermediate temperature for all the Fe(II) ions. Since the Fe(II) ions are coordinated to the central anion and to three framework oxygens which can belong to SiO_4 or BeO_4 tetrahedra, there are different possible configurations (for example

Table 1 Mössbauer parameters obtained from the fit of the room temperature spectra

	$Fe_8[BeSiO_4]_6S_2$	$Fe_8[BeSiO_4]_6Se_2$	Zn_4Fe_4 $BeSiO_4]_6S_2$	$Fe_4Mn_4[BeSiO_4]_6S_2$
Main absorption				
$\delta(\pm 0.01(mms^{-1}))$	0.93	0.93	0.93	0.94
$\Delta E_Q(\pm 0.02\ (mms^{-1}))$	0	0.33	0.26	0.24
FWHM ($\pm$ 0.02 (mms^{-1}))	0.36	0.30	0.33	0.34
Area ($\pm$ 2 (%))	97	97	96	100[a]
Impurity phase				
$\delta(\pm 0.01\ (mms^{-1}))$	1.13	1.09	1.11	
ΔE_Q ($\pm$ 0.02 (mms^{-1}))	2.85	2.73	2.83	
FWHM ($\pm$ 0.02 (mms^{-1}))	0.24	0.36	0.25	
Area ($\pm$ 2 (%))	3	3	4	

[a]Although the spectrum has been only fitted to a quadrupole doublet close inspection of the figure indicated that an impurity phase is also present

all the oxygens belonging to SiO_4 tetrahedra, or two oxygens belonging to SiO_4 tetrahedra and the other to 1 BeO_4 tetrahedra, etcetera) which can be in the origin of the small differences observed. Because of the existence of this quadrupole splitting distribution a fitting model involving only a couple of discrete lines gave unsatisfactory results. Therefore, all the low-temperature spectra were fitted to a histogram of quadrupole doublets without any predetermined shape for the distribution. Hence, all the quadrupole splitting values quoted in this paper for the low-temperature spectra correspond to the average value of the distribution. The obtained values at the different temperatures for the different samples are shown in Fig. 7. The experimental data in Fig. 7 were fitted using the expression:

$$\Delta E_Q = \Delta E_Q(0)\frac{1-\exp\left(-\frac{\Delta}{kT}\right)}{1+\exp\left(-\frac{\Delta}{kT}\right)} + \Delta E_Q(lattice) \quad (1)$$

where k is the Boltzmann constant, $\Delta E_Q(0)$ is the quadrupole splitting at T = 0 K, Δ is the separation between the two e_g states of the Fe(II) ion and ΔE_Q(lattice) is a constant term which accounts for the lattice contribution to the electric field gradient. It is worth noting that to obtain a curve which fits well the experimental data it is necessary to include this constant lattice term. The resulting curves are also depicted in Fig. 7. In general, the values are small and close to the 50 cm^{-1} value reported for the above-mentioned natural dalanite sample (46.3 cm^{-1}, 55.5 cm^{-1}, 58.2 cm^{-1} and 52.9 cm^{-1} for $Fe_8[BeSiO_4]_6S_2$, $Fe_8[BeSiO_4]_6Se_2$, $Zn_4Fe_4[BeSiO_4]_6S_2$ and $Fe_4Mn_4[BeSiO_4]_6S_2$, respectively). It must be also be pointed out that because of the existence of the quadrupole splitting distributions the calculated Δ values correspond consequently to average values.

The present work also demonstrates the sensitivity of the Mössbauer parameters to changes in the environment of iron beyond its first coordination shell (i.e. Zn/Mn instead of Fe) when its immediate coordination remains unchanged. It is noteworthy that the synthetic mixed cation samples $Fe_4Mn_4[BeSiO_4]_6S_2$ and $Fe_4Zn_4[BeSiO_4]_6S_2$ both showed a small quadrupole splitting at room temperature, in agreement with the natural mineral sample. The temperature-dependent quadrupole splitting behaviour for the natural and synthetic danalite samples is entirely consistent with Mössbauer spectra observed for other tetrahedral iron(II) materials, where a small splitting of the e levels is expected due to loss of symmetry (either due to the constraints of the crystal structure, as in $[NMe_4]_2FeCl_4$ [8] or

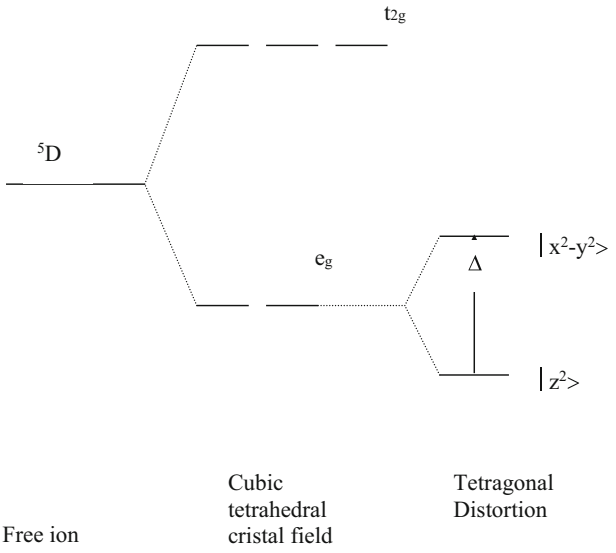

Fig. 4 Splitting of the energy levels of Fe(II) in the tetrahedral coordination by the crystal field interations in the presence of tetragonal distortion

as a result of slightly different groups surrounding the iron centre); at room temperature the material possesses enough thermal energy to allow electrons to populate both e_g levels, which reduces the valence contribution to the EFG. Substitution of the sulfide by selenide results in a quadrupole split doublet at room temperature where the lattice contribution can no longer overcome the valence contribution. As the difference in bonding character between the oxides and chalcogenide increases, the splitting of the e_g levels is accentuated and a larger electric field gradient is observed.

Isotherms as a function of applied field are shown in Fig. 8 and are characterised by a temperature dependent slope in the high field region (above 1 Tesla). The low field region exhibits a strong field dependence resembling saturation of some of the magnetic contribution in relatively low applied fields.

The most likely explanation for this is the presence of the small amount of ferromagnetic fayalite that was observed in the Mössbauer data. Formerly [3], this was tentatively interpreted as the presence of ferromagnetically coupled clusters. Such an assumption could account for the magnetisation behaviour in low applied fields as such a contribution would be aligned easily and be saturated in relatively low external magnetic fields. However, the impurity explanation is confirmed by the low temperature neutron diffraction data, which shows no evidence of the three-dimensional ferromagnetic ordering in the sulphide sample; *vide infra*.

Analysis of the high field part of the magnetisation curves and the susceptibility extracted from this data reveals that the high field inverse susceptibility follows a Curie-Weiss law (Fig. 9). Fitting of the straight line yields an effective paramagnetic moment of 4.53 μ_B/Fe-atom in good agreement with a high spin d^6 Fe-ion with four unpaired electrons. The paramagnetic Curie temperature is approximately –160 K suggesting that interactions within the clusters are predominately antiferromagnetic in nature. The much weaker interactions between the metal clusters in comparison to interactions within the clusters, are

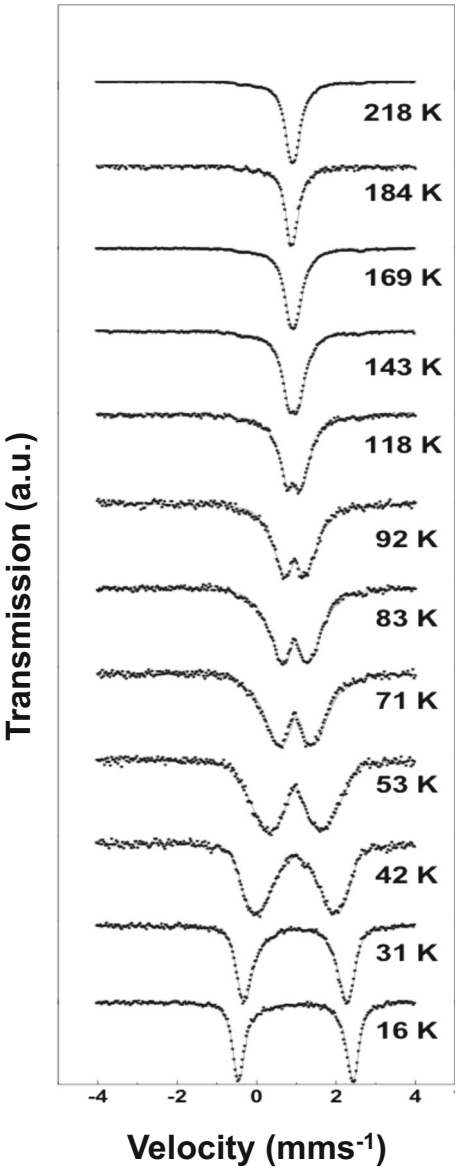

Fig. 5 Low temperature Mössbauer spectra recorded from $Fe_8[BeSiO_4]_6S_2$

probably due to the much larger interatomic separation (4 Å (iron to iron) vs 7 Å between the centres of the metal clusters).

Paramagnetic scattering and magnetic order of $Fe_8(BeSiO_4)_6X_2$, X = S, Se was investigated as a function of temperature by collecting neutron scattering data between 200 and 2 K.

Figure 10 shows the variation of the magnetic cross-section as a function of scattering vector at 200 K. The scattering is essentially determined by the magnetic form factor. This implies that the magnetic moments of the Fe atoms in the cluster are not magnetically correlated, i.e. they are in a paramagnetic state (each magnetic moment moves independently

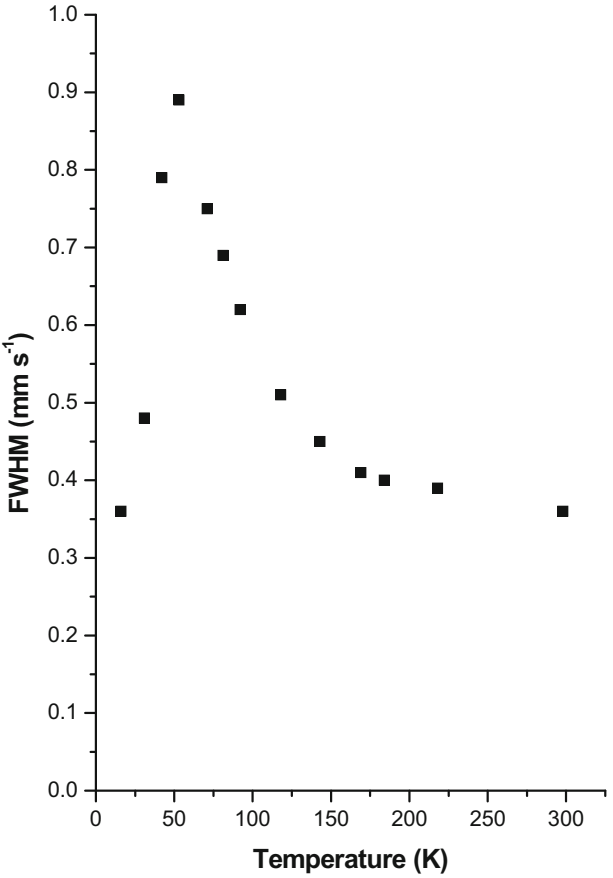

Fig. 6 Linewidth variation with temperature of the Mössbauer spectra recorded from $Fe_8[BeSiO_4]_6S_2$

of its neighbours) resulting in a scattering vector (Q) independent scattering contribution. The only Q-dependence arises due to the magnetic form factor of the magnetic moment of the Fe^{2+} ion. Figure 11 summarises the data sets collected between 50 and 5 K and shows that there is little difference in the form of the data over this temperature range. No long-range magnetic order is present as evidenced from the absence of peaks in the scattering cross-section. However comparison of the 200 K and 50 K data sets, Fig. 12, shows that on reaching 50 K $Fe_8(BeSiO_4)_6Se_2$ is no longer totally paramagnetic.

As the temperature is lowered, predominately antiferromagnetic correlations set in. This is reflected in the magnetic scattering by a reduction of the magnetic intensity in the forward direction combined with an enhancement of the magnetic scattering at those distances (determined by 2π/(nearest Fe-atom distance in cluster) in units of $Å^{-1}$). In $Fe_8(BeSiO_4)_6Se_2$ this distance is approximately 1.35 $Å^{-1}$ corresponding to an Fe-Fe distance in the cluster of ~4.5 Å.

On reduction of the temperature in the range 50–5 K, the forward scattering (i.e. the scattering at small Q-values) decreases. This implies that the magnetic correlations become stronger and more antiferromagnetic. However, the magnetic scattering at $Q = 0$ does not

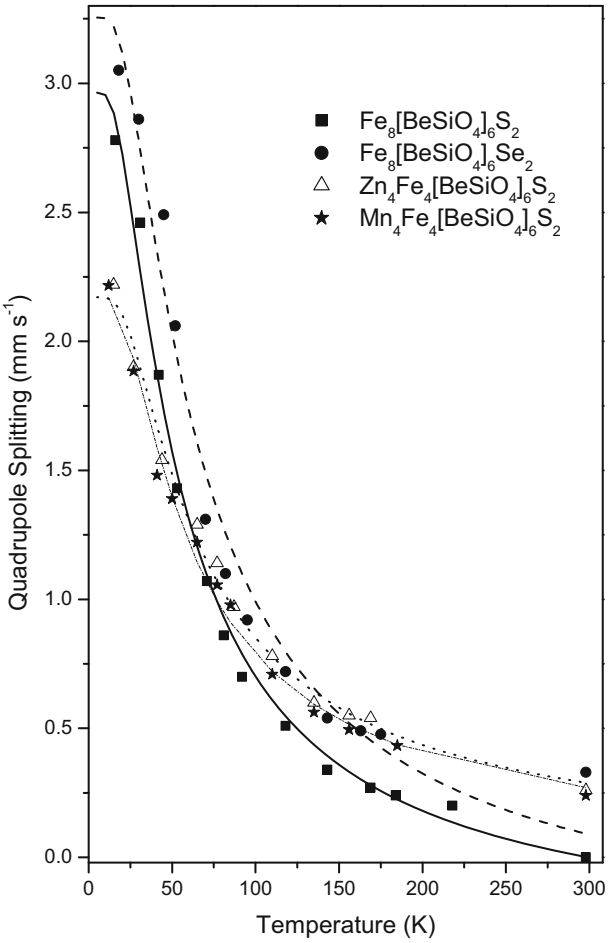

Fig. 7 Temperature dependence of the quadrupole splitting of the different samples. The dots correspond to the average value of the quadrupole dstributions used to fit the spectra. The lines represent the fir of equation [1] to the data

tend to zero as it would for a perfect antiferromagnet. This implies that the magnetic correlations have a ferromagnetic component to it, between the clusters such that there is an overall moment on the cluster. This in turn suggests a canted arrangement of magnetic moments in the cluster. In view of the geometrical arrangement of Fe-moments in the form of a pyramid (which potentially gives rise to magnetic frustration) this is not surprising. The magnetic moments are most likely arranged in a non-collinear manner.

At T = 2 K three-dimensional magnetic order is observed in $Fe_8(BeSiO_4)_6Se_2$, see Figs. 13 and 14. Magnetic Bragg reflections occur at positions for which enhancement has been observed at higher temperatures. Note the change in scale on the onset of magnetic long-range order and that the magnetic short-range order displayed by the clusters does not completely disappear when long-range magnetic order sets in. This implies that the ordered moment is smaller than the full moment located on the Fe-atom. A significant disordered part of the moment remains. This, however, is still correlated within a single cluster. Such an

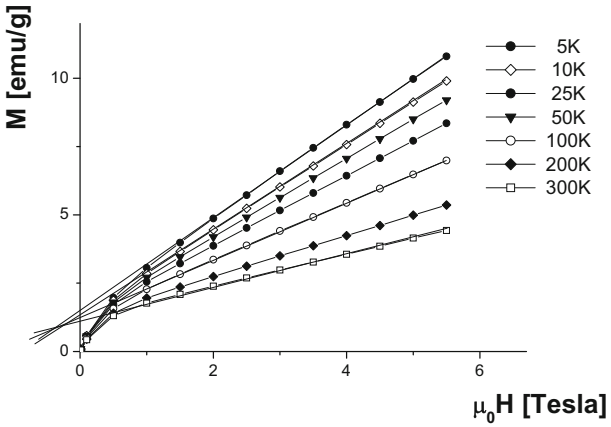

Fig. 8 Isotherms as a function of applied field for $Fe_8[BeSiO_4]_6S_2$

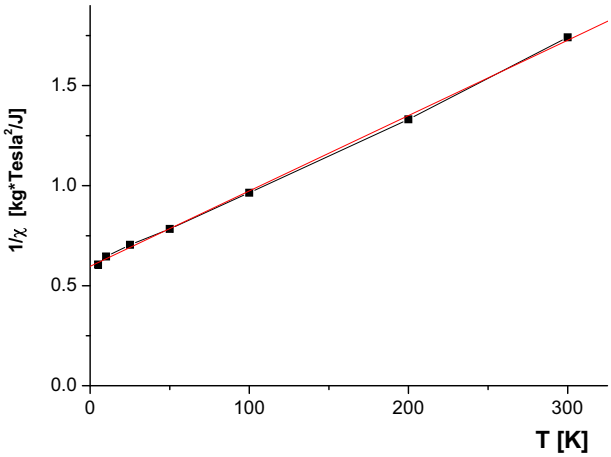

Fig. 9 Curie-Weiss plot of the molar susceptibility (high field) of $Fe_8[BeSiO_4]_6S_2$

observation is entirely consistent with the notion of magnetic frustration, which implies that a large number of different magnetic configurations have very similar energy. The magnetic order does not select a unique ground state, but only partially lifts the degeneracy resulting in a significant contribution to the magnetic scattering from the non-ordered (fluctuating) part of the magnetic moment (Fig. 14).

Data were collected from $Fe_8(BeSiO_4)_6S_2$ at a series of temperatures between 250 and 1.5 K and are presented in Fig. 15. In contrast to the Se data presented previously, no magnetic Bragg reflection is visible even in the lowest temperature data set implying that unlike $Fe_8(BeSiO_4)_6Se_2$, $Fe_8(BeSiO_4)_6S_2$ does not order magnetically in three-dimensions even at 2 K. For all the data sets between 250 and 1.5 K a broad feature is again visible near $Q = 1.2$ Å^{-1}, expected for an antiferromagnetic cluster with an Fe-Fe correlation distance near 5 Å. Inspection of the shape of the curve at low Q values which again turns down towards $Q = 0$ indicates anti-ferromagnetic correlations.

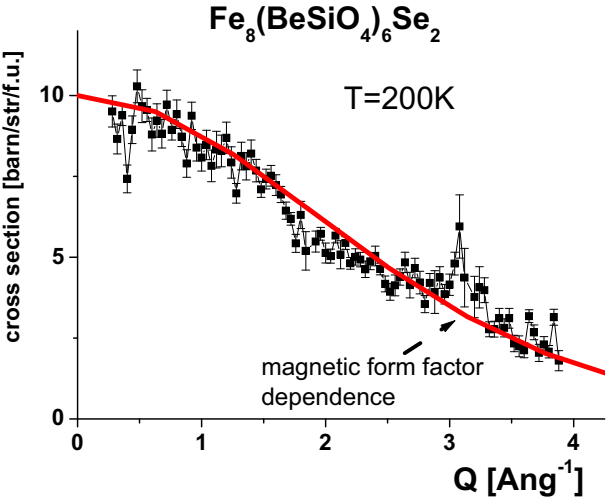

Fig. 10 Variation of magnetic scattering cross-section in as a function of Q in $Fe_8(BeSiO_4)_6Se_2$ at 200 K

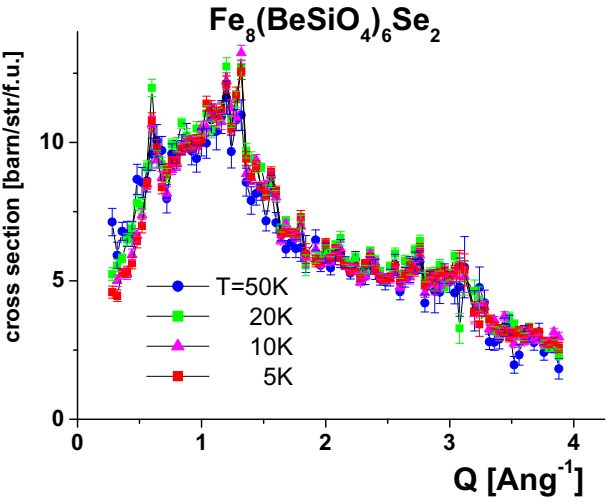

Fig. 11 Variation of magnetic scattering cross-section as a function of Q in $Fe_8(BeSiO_4)_6Se_2$ at 50, 20, 10 and 5 K

Analysis of the Mössbauer data from $Fe_8(BeSiO_4)_6S_2$ has shown that the origin of the effectively zero observed quadrupole splitting in material is the equivalence (and opposite influence) of the lattice and valence contributions. This suggests that the separation Δ, Fig. 4, between the two e_g states brought about by the elongated tetrahedron is extremely small giving a small valence splitting contribution to the ΔE_Q which is this readily compensated for by the lattice contribution. Replacement of S by Se, as in $Fe_8(BeSiO_4)_6Se_2$, has been found to lead to a larger quadrupole splitting in the Mössbauer which would infer a larger valence contribution. Given the increased asymmetry of the FeO_3X co-ordination

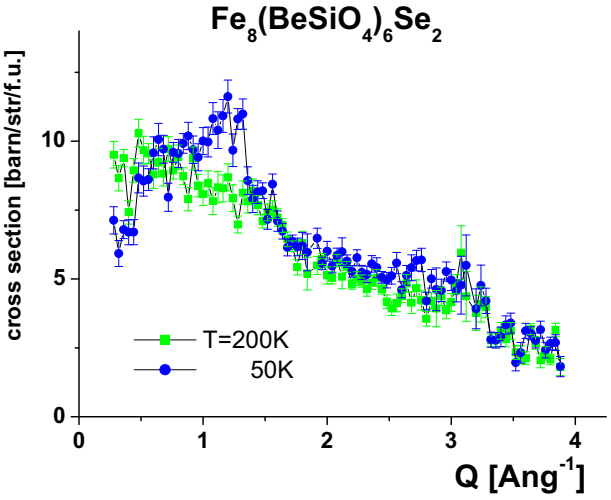

Fig. 12 Comparison of the variation of the magnetic scattering cross-section as a function of Q in $Fe_8(BeSiO_4)_6Se_2$ at 200 and 50 K

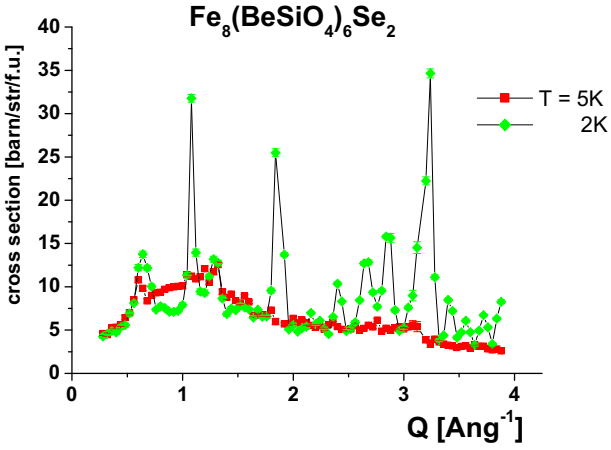

Fig. 13 Comparison of the variation of the magnetic scattering cross-section as a function of Q in $Fe_8[BeSiO_4]_6Se_2$ at 5 K and 2 K. Full scale

tetrahedron as Se replaces S [3] this change is not unexpected. The low temperature Mössbauer obtained from $Fe_8(BeSiO_4)_6S_2$ show an increased quadrupole splitting compared with that at room temperature. Whilst the lattice contribution is largely independent of temperature, the valence contribution increases as the temperature falls. Analysis of the data as a function of temperature shows that this dominance is apparent for all phases prepared. The data for the $Fe_8(BeSiO_4)_6S_2$ and $Fe_8(BeSiO_4)_6Se_2$ trace almost identical curves indicating that the valence contribution is identical as expected, however the absolute value is shifted by the lattice contribution which differs due to the change in chalcogenide.

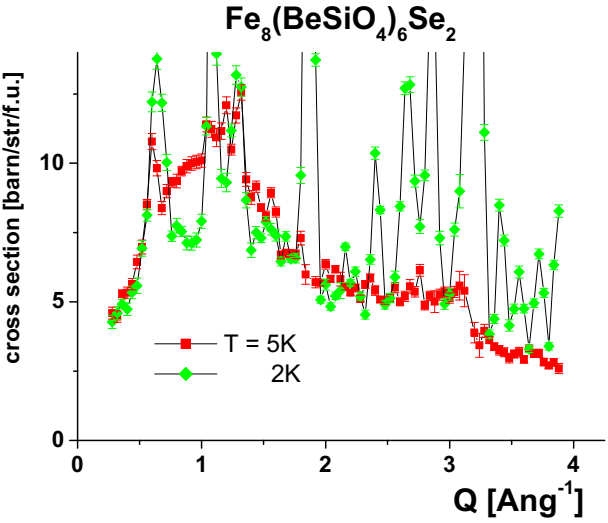

Fig. 14 Comparison of the variation of the magnetic scattering cross-section in as a function of Q in $Fe_8(BeSiO_4)_6Se_2$ at 5 K and 2 K. Expanded data for low cross-sections

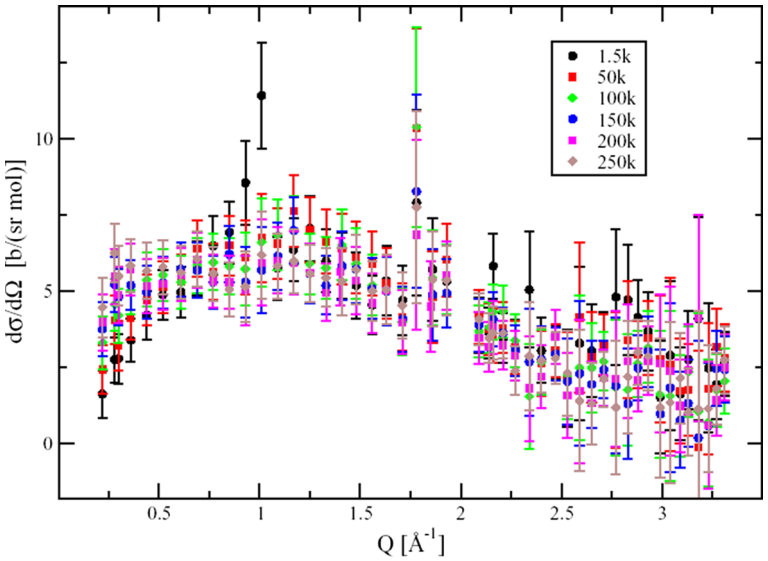

Fig. 15 Variation of the magnetic scattering cross-section as a function of Q for $Fe_8(BeSiO_4)_6Se_2$ between 250 and 1.5 K

Analysis of the quadrupole splitting as a function of temperature gave a value for the crystal field splitting of only 52.9 cm^{-1}. This value is slightly larger than the value calculated by Maeda et al. [7] for the danalite minerals that contained a mixture of cations (Fe, Mn, Ca, Zn). Scrutiny of the data from the mixed cation samples show a slightly different

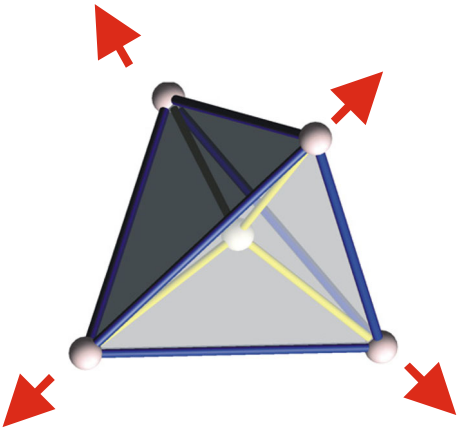

Fig. 16 Possible spin orientation geometry for the frustrated Fe_4X cluster

variation with temperature and these samples are more similar to the mineral samples. It is perhaps therefore not surprising that there is a slight variation in the value of Δ calculated.

None of Mössbauer spectra shows any evidence of long range magnetic ordering down to 16 K and any local ordering, i.e. within an individual Fe_4X trapped unit, would not be expected to affect the form of the Mössbauer data. It was not possible to collect Mössbauer data below 2 K where long range magnetic ordering was observed in the neutron scattering experiments for $Fe_8(BeSiO_4)_6Se_2$ though the danalite mineral, studied in detail by Mössbauer, shows no long range magnetic ordering even at 1.5 K. However the neutron scattering studies were able to shed some light on the local magnetic ordering in these materials.

Both $Fe_8(BeSiO_4)_6Se_2$ and $Fe_8(BeSiO_4)_6S_2$ show evidence for magnetic correlations on a length scale of around 4–5 Å below room temperature, though it is noteworthy that for the sulphide these correlations are apparent at 250 K while for the selenide they appear between 200 and 50 K. These magnetic interactions seem to be mainly anti-ferromagnetic in nature but the cluster has a canted spin arrangement rather than being perfectly anti-ferromagnetic. As noted above, the tetrahedral geometry of the Fe_4X cluster precludes perfect antiferromagnetic ordering and the frustration in such systems often leads to canted spin arrangements. A possible spin orientation geometry is shown in Fig. 16 and has spin orientations aligned at 109.8° to each other.

The strength of the Fe-Fe magnetic correlations within the cluster is likely to depend on the Fe-Fe separation and /or the strength of the linking Fe-X-Fe bonds. The latter is probably of most importance, particularly if a superexchange type mechanism involving the atomic orbitals on X is responsible. Regardless of mechanism, these interactions will be strongest for sulphur in $Fe_8(BeSiO_4)_6S_2$ which has the shortest Fe-X bonds and shorter intra-tetrahedral Fe-Fe distance—see Fig. 17. This is presumably the origin of the fact that the ***local*** magnetic correlations are seen near room temperature in $Fe_8(BeSiO_4)_6S_2$ but at lower temperatures for $Fe_8(BeSiO_4)_6Se_2$.

However long-range magnetic ordering is seen at 2 K for the selenide, but not for the sulphide. The three dimensional ordering requires interactions between iron atoms in neighbouring sodalite cages. These interactions are likely to be through space or possibly (but less likely) involve a super-exchange mechanism though the framework oxygen. Figure 17 also plots this intercage Fe-Fe distance as a function of chalcogenide where it can be seen to decrease with increasing chalcogenide anion size. These intercage magnetic interactions

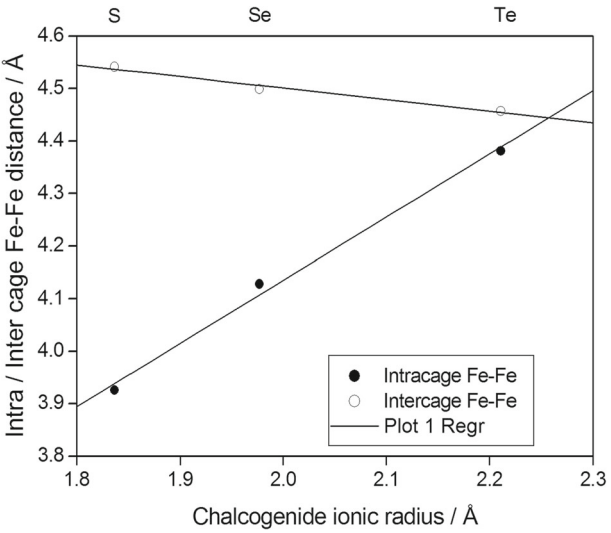

Fig. 17 Variation in intra- and inter- cage Fe-Fe distances as a function of Chalcogenide ion size for $Fe_8(BeSiO_4)_6Se_2$

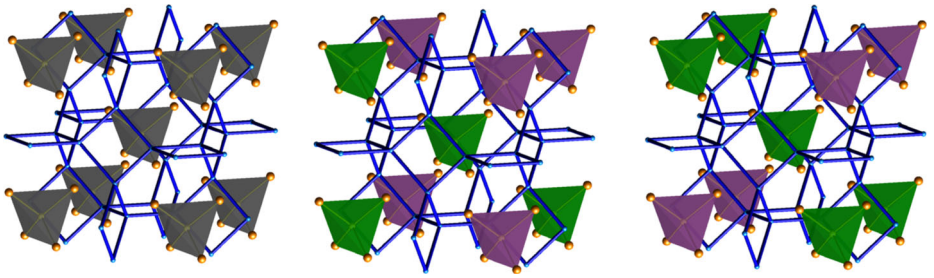

Fig. 18 Representation of magnetic correlations in $Fe_8(BeSiO_4)_6Se_2$ as a function of temperature. *Left*.- grey tetrahedra represent paramagnetic state; *centre*.- individual tetrahedra have some magnetic correlations (green and purple tetrahedra represent different possible spin orientations in the frustrated arrangement); *right*.- a possible three dimensionally magnetically ordered arrangement of individual tetrahedra

would be expected to become stronger with increasing lanthanide size a result borne out by the observation that $Fe_8(BeSiO_4)_6Se_2$ is magnetically three dimensionally ordered at 2 K while $Fe_8(BeSiO_4)_6Se_2$ is not.

The danalite series of materials may thus be considered to be framework expanded frustrated nanomagnets in that individual tetrahedral Fe_4X units are separated in an ordered array by a beryllosilicate framework. At high temperatures these nanounits are individual paramagnets, Fig. 18 left, but on cooling below room temperature magnetic correlations form within the nanounits but there is no communication between neighbouring sodalite cages, Fig. 18 centre. At very low temperatures in $Fe_8(BeSiO_4)_6Se_2$ the individual units develop three dimensional order, Fig. 18 right, though the true magnetic structure of this material will require further detailed analysis of the low temperature magnetic Bragg diffraction.

4 Conclusions

We have characterised by Mössbauer spectroscopy and magnetic measurements a series of synthetic helvite analogues $Fe_4M_4[BeSiO_4]_6X_2$ (M = Fe, Mn; X = S, Se). The Mössbauer data have shown that iron is present as high spin Fe(II) in tetrahedral coordination. At room temperature the valence contribution to the electric field gradient is almost compensated by the lattice contribution. From the dependence of the quadrupole splitting at room temperature the energy separation Δ between the two e_g levels originated by the occurrence of tetragonal distortion has been determined for all the samples. The values obtained are relatively small: they vary between 45 and 60 cm^{-1} and are within the range of those observed in natural dalanite samples. The Mössbauer spectra only show paramagnetic singlets/doublets in all the range of temperatures considered. The lack of long-range magnetic order observed by Mössbauer spectroscopy agrees with the neutron diffraction data which suggest that the M_4X units are largely magnetically isolated within their cages leading to a frustrated magnet with no long range interaction for the sulfide species.

References

1. Barth, T.F.W.: Norsk Geol. Tidsskr. **9**, 40 (1926)
2. Mel'nikov, O.K., Latvin, B.M., Fedosova, S.P.: Gidroterm. Sint. Krist. **167** (1968)
3. Armstrong, J.A., Dann, S.E., Neumann, K.U., Marco, J.F.: J. Mater. Chem. **13**, 1229 (2003)
4. Dann, S.E., Weller, M.T., Rainford, B.D., Adroja, D.T.: Inorg. Chem. **36**, 5278 (1997)
5. Edwards, P.R., Johnson, C.E., Williams, R.J.P.: J. Chem. Phys. **47**, 2074 (1967)
6. Ingalls, R.: Phys. Rev. **133**, A787 (1964)
7. Maeda, Y., Takashima, Y., Ishida, K.: Bull. Chem. Soc. Jpn. **58**, 1047 (1985)
8. Srivastave, K.K.P., Choudhary, S.N.: Phys. Stat. Solidi B **1**, 289 (1986)